Journal of Civil Engineering, Science and Technology
*Volume 15, Issue 1, April 2024, 69-77*

# A NOVEL APPROACH OF NON-DESTRUCTIVE TESTING FOR W-BEAM GUARDRAIL DEFECT DETECTION USING SURFACE WAVE TECHNOLOGY

Muhammad Rasyadi Yusof Zaki and Syamsul Bahrin Abdul Hamid*
Kulliyyah of Engineering, International Islamic University Malaysia, 53100 Selangor, Malaysia

Date received: 06/08/2023 Date accepted: 25/03/2024
*Corresponding author's email: syamsul_bahrin@iium.edu.my
DOI: 10.33736/jcest.5916.2024

***Abstract*** — The W-beam guardrail, alternatively referred to as a guardrail or railing, constitutes a system meticulously engineered to prevent vehicular deviation into hazardous or restricted zones. Such mechanisms are ubiquitously employed across major global thoroughfares. However, vehicular collisions can inflict considerable damage upon the W-beam, thereby compromising its structural integrity. Concurrently, subpar maintenance further exacerbates this issue, potentially transforming the W-beam from an accident prevention tool into a catalyst for mishaps. Hence, the implementation of an effective maintenance and inspection strategy is imperative. The research presented herein proposes a novel method for W-beam defect detection, leveraging surface wave technology. A pulse-echo setup has been established, employing a 10-cycle tone burst to operate at a centre frequency of 48 kHz as the transmission medium. Signals reflected from the defective specimen were subsequently analysed; however, it was observed that this technique was unable to detect all defects. Despite these limitations, the study delineates the potential to pinpoint the precise location of physical hole defects. This was achieved through the time-of-flight method and leveraging known material characteristics, such as the speed of sound, at 5 cm between the hole and transmitter. The researchers predict that this methodology, when augmented with a higher voltage and a suitable amplifier circuit for detection, could be utilized for long-distance defect detection. This opens up new avenues for ensuring the structural integrity of W-beam guardrails, thereby enhancing road safety.



***Keywords*:** defect detection, ultrasonic, guardrail, transport, road safety, measurement

## 1.0 INTRODUCTION

The pivotal role of transportation infrastructure in contemporary societies, specifically in facilitating the expeditious transportation of individuals and goods, cannot be underestimated. W-beam guardrails serve as integral constituents of this infrastructure due to their widespread deployment as safety barricades designed to alleviate the harshness of road accidents, thereby safeguarding motorists [1–3]. Consequently, the assurance of their structural integrity [4] and overall health [1, 5] is a critical factor in the preservation of road safety. A myriad of damages, for instance, material degradation [6], corrosion [4], or cracks [7], could severely undermine the effectiveness of these guardrails, potentially culminating in disastrous outcomes. This article introduces an innovative method for identifying W-beam damages by exploiting the potentials of Ultrasonic Surface Wave (USW) [8, 9] technology to non-destructively and accurately evaluate the condition of W-beam guardrails.

The current landscape of W-beam guardrail inspection is fraught with challenges. Conventional inspection techniques often involve manual testing or visual inspections [10], both of which are labour-intensive, time-consuming, and may not offer a comprehensive evaluation of concealed defects [11]. Additionally, these methods frequently expose inspectors to safety hazards, notably during the inspection of elevated structures or high-traffic regions [12]. The growing demand for advanced, efficient inspection techniques capable of promptly and accurately identifying structural abnormalities and W-beam damages underscores the urgency for timely maintenance and effective safety interventions. USW technology has gained traction as a powerful instrument for non-destructive evaluation across diverse engineering applications [13–16]. The technology operates by propagating along the surface of a material, hence, its heightened sensitivity and resolution for detecting near-surface defects [17]. This distinctive trait positions USW as the optimal solution for inspecting structures like W-beam guardrails, where surface damages or defects are the primary concern.

The motivation underpinning this research is the quest to enhance the inspection process for W-beam guardrails by offering a reliable, rapid, non-invasive technique for damage detection. The goal is to harness USW technology to develop an automated, efficient inspection system capable of identifying various damage types, including but not limited to cracks, corrosion, and material degradation, even when they are not surface-visible. The overarching objective is to augment the safety of transportation infrastructure by facilitating the early detection and efficient maintenance of W-beam guardrails, thereby diminishing potential risks to road users.

The key contributions of this research encapsulate the development of a USW-based inspection system, where we illustrate the design and implementation of an innovative inspection system leveraging on USW technology to detect and characterize W-beam guardrail damages. The proposed system provides the possibility of automation and real-time data acquisition, thereby ensuring rapid assessment and diminishing the necessity for manual interventions. By capitalizing on the potentials of USW, the inspection system delivers enhanced accuracy and sensitivity, thereby enabling the detection of hidden defects potentially overlooked by visual inspections. The non-destructive nature of USW inspection guarantees that the structural integrity of the W-beams remains intact, hence prioritizing the safety of inspectors.

## 2.0 METHODOLOGY

### 2.1. Detection of Flaw Using Ultrasonic

The ultrasonic inspection system, in its most comprehensive form, is comprised of one or more transducer probes, supplemented by peripheral apparatus including display devices and a pulser/receiver unit. The pulser/receiver is an electronic instrument capable of generating high-voltage electrical pulses. Upon receipt of these pulses, the transducer converts them into high-frequency ultrasonic energy. This energy, in the form of sound waves, then propagates through various materials. When a discontinuity - such as a crack - interrupts the path of these waves, a portion of the energy is reflected off the defect's surface. The reflected wave oscillation is then converted back into an electrical signal via the transducer's transduction process, which can be visually represented on a display screen.

The system is then used to scan or detect abnormalities within a specimen. An appropriate coupling method is employed to diminish impedance mismatch, enabling a more substantial amount of sound energy to permeate the specimen. This results in a heightened sensitivity and thus a more usable ultrasonic signal. The process of flaw detection requires careful consideration of a few key elements, including the detection, location, evaluation, and diagnosis of reflectors.

Rather than using the term 'reflector', ultrasonic operators often prefer 'discontinuity' to minimise ambiguity in communication. A discontinuity is defined as an irregularity within the test object which is suspected to be a flaw. The determination of whether a discontinuity constitutes a flaw affecting the test object's purpose can only be made following location, evaluation, and diagnosis. The primary objective of the method under discussion is to pinpoint an effective technique capable of detecting discontinuities over short distances in a laboratory setting, with the potential for application over longer distances typical of W-beams used in Malaysian roads. Consequently, the setup should be arranged to facilitate the use of a single probe, with surface wave propagation technique enabling such long-distance defect detection.

### 2.2. Experimental Setup

The experimental setup, as depicted in Figure 1, encompasses two function generators, an oscilloscope, a power supply, and a solitary transducer functioning as the primary probe to facilitate the detection of defects within the specimen. The function generators were configured in a specific manner, with one generating a sequence of 10 pulses at a frequency of 48 kHz. Concurrently, the second function generator was tasked with synchronizing the entire system at an approximate interval of 10 kHz.

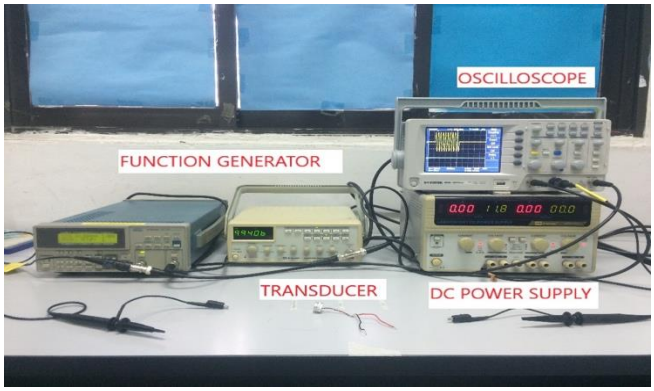


**Figure 1** Experiment setup

In this study, an exploration of surface waves, which traverse the exterior of a relatively dense solid substance penetrating to a depth equivalent to one wavelength, is conducted. The choice of surface waves in this investigation holds significant value due to their ability to cover substantial distances in comparison to other wave types. To decipher an appropriate activation angle that would facilitate optimal generation of these surface waves, Snell's Law is employed, as demonstrated in Figure 2 (Left). In order to facilitate the generation of the surface wave, it is imperative that the refracted angle, denoted as $\theta_2$, is precisely at 90°. This crucial aspect is graphically represented and further elucidated in the following Figure 2 (Right).

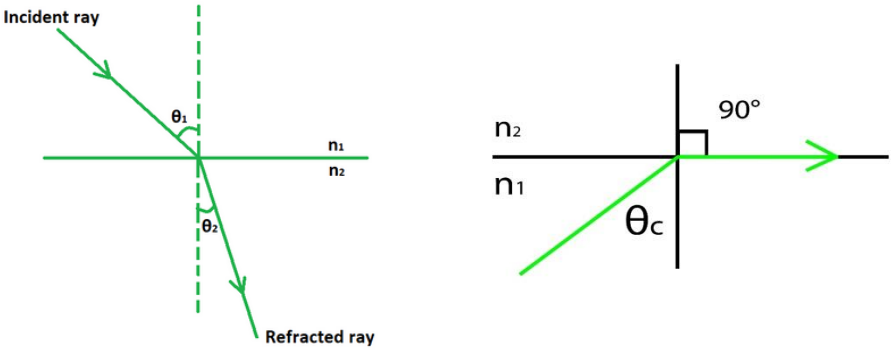


**Figure 2** The law of refraction or Snell's law (Left). Angle of incidence equal to critical angle (right)

Snell's Law is utilized to calculate the angle of refraction, specifically aiming to achieve an incidence angle of 90°, exemplified in Equation 1:

$$n_1 \sin\theta_1 = n_2 \sin\theta_2 \tag{1}$$

Equation 1 can be arranged in terms of the velocity as shown in Equation 2:

$$\frac{\sin\theta_1}{\sin\theta_2} = \frac{v_1}{v_2} \tag{2}$$

According to Equation 2, it is imperative that $\theta_2$ be positioned at a 90° angle to facilitate the transverse refraction across the surface. This is due to the wave propagation that is expected to traverse two distinct materials emanating from the transducer probe. Therefore, it is crucial to determine the specific speed of sound in these materials. The ultrasonic wave is designed to propagate via an angle beam composed of Acrylonitrile Butadiene Styrene (ABS), subsequently passing through the W-beam constructed from aluminium. By manipulating Equation 2, it is possible to discern the incident angle, $\theta_1$, which subsequently leads us to Equation 3:

$$\sin\theta_1 = \frac{2230}{6300}\sin 90° \tag{3}$$

The speed of sound in Acrylonitrile Butane Styrene (ABS) [18], $v_1$ is 2230 $ms^{-1}$ and speed of sound in aluminium, $v_2$ is 6300 $ms^{-1}$[19].

Derived from Equation 3, the calculated value of $\theta_1$ subsequently equates to 20.7°. In order to engender the requisite surface wave, a triangular prism has been meticulously fabricated via the advanced technique of rapid prototyping, incorporating an angle of 20.7°, a depiction of which is exhibited in Figure 3 (left). This triangular prism is designed to function as a conduit, directing the propagation of the ultrasonic wave. The orthogonal perspective of the aforementioned triangular prism can be visualized in Figure 3 (right).

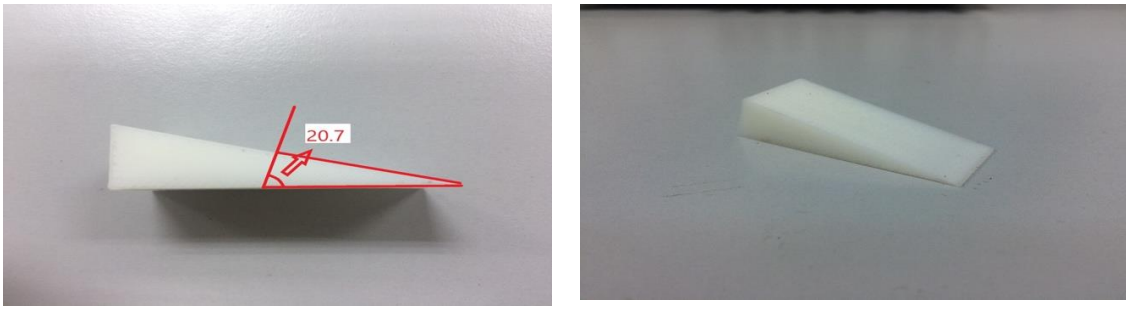


**Figure 3** The angle of reflection in ABS plastic (Left). Orthogonal view of the angle block beam (Right)

In the center of the triangular prism, a Multicom 48 kHz Transducer is strategically positioned. It is affixed at a distance of precisely 10 mm from the edge of the guard rail, utilizing a coupling gel as the attachment medium. The purpose of this particular placement and method is to mitigate the impedance mismatch that could occur between the transducer and the w-beam. Any potential mismatch could result in significant energy loss to the surrounding environment, as depicted in Figure 4.

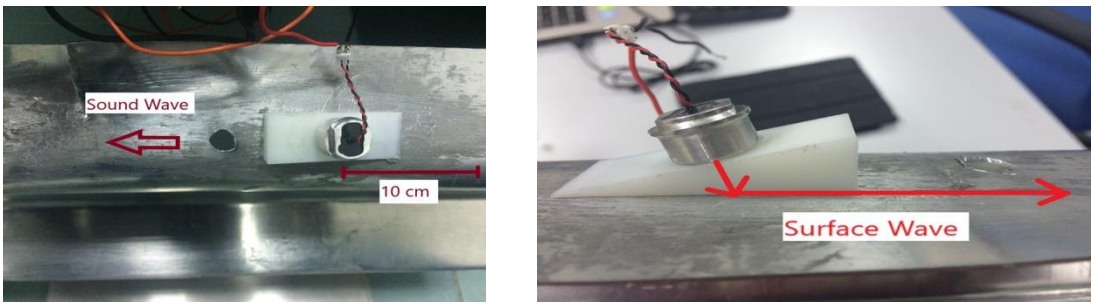


**Figure 4** Placement of angle beam block and transducer on the guard rail. Top View (Left) Side View (Right)

In the given experimental procedure, the coupling gel of brand D Olympus is employed as an intermediary medium to facilitate the transmission process between various components, namely the transducer, angle beam block, and guard rail. The strategic positioning of the transducer, at a distance of 15 cm from the guard rail's edge, is intended to generate a discernible reflection difference. The function generator is configured to transmit a 10 cycle tone burst, with a centrally located frequency of 48 kHz. Figure 4 (right) provides a visual representation of the setup employed for the activation along with the anticipated direction of the resultant surface wave. Upon placement of the transducer on the angle beam block, it is hypothesized that the transmitted signal will reflect at an angle of 20.7 degrees, thereby instigating the generation of the requisite surface wave, oriented in the direction denoted in red. The propagation of the surface wave persists along the guard rail until it encounters either the termination point of the rail, at which juncture reflection occurs, or the presence of a defect. The subsequent reception signal is subsequently manifested on the oscilloscope for further analysis and interpretation.

## 3.0 RESULTS AND DISCUSSION

### 3.1. Defect Detection

#### *3.1.1. No load*

The experimental approach employed in this study hinges on the pulse and echo method. As such, it is anticipated that there will be a delay before the echo signal is received, due to the inherent time-of-flight. Figure 5 presents the transmitted signal on Channel 1, characterized by a 10 cycle tone burst at a centre frequency of 48 kHz, generated by a Sony AFG-310 Arbitrary Function Generator. Channel 2 of the same figure displays the transmission of an identical tone burst signal when engaged with a transducer operating at 48 kHz. Presently, the transducer is not situated on the guard rail, yet a noticeable reverberation is detectable within the transducer.

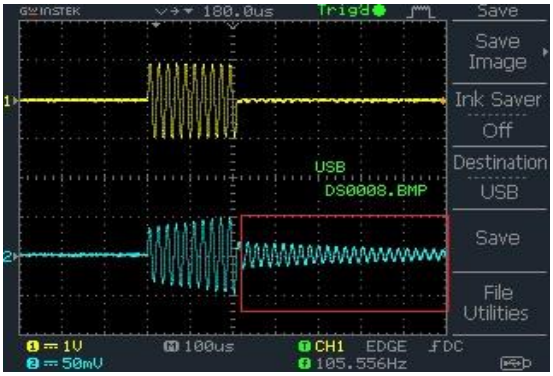


**Figure 5** Tone burst signal generated by the function generator shown by the oscilloscope

#### *3.1.2. No defect*

The transmission of the signal will persist until it reaches the termination point of the guard rail, operating at a frequency of 48 kHz. Should the signal discern no irregularities throughout its journey to the periphery of the w-beam, a reflection of the signal will occur. This reflection will be identical in frequency to the initial transmission, maintaining a frequency of 48 kHz at the guard rail's endpoint. As depicted in Figure 6, both the commencement and the culmination of the guard rail are clearly demarcated.

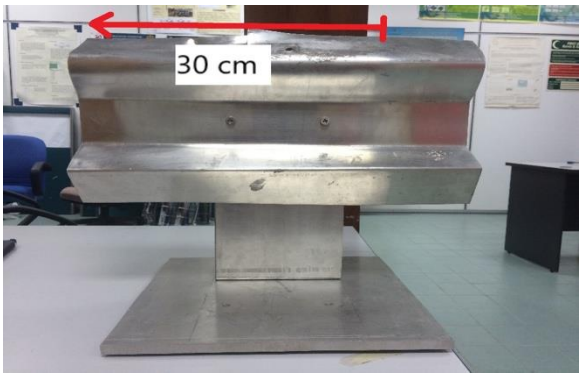


**Figure 6** The signal will be reflected at the end of the guard rail

As presented in Figure 6, the signal traverses a total distance of 60 cm; this includes a 30 cm transmission distance and an equivalent reflection distance from the terminal of the guard rail. Consequently, a minor phase discrepancy is discernible between the transmitted and received signals. Additionally, Figure 7 also illustrates the absence of a reflection signal, which is attributable to the lack of detected defects across the entire beam.

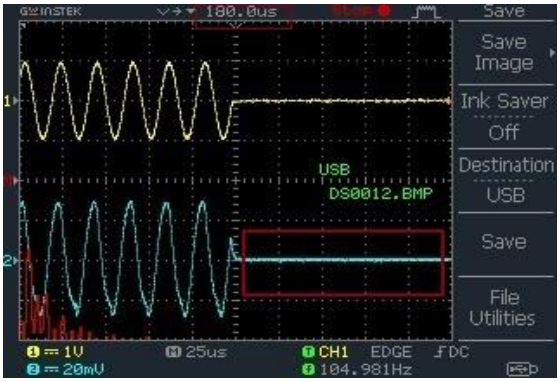


**Figure 7** No reflection signal is plotted on the oscilloscope

*3.1.3. With defect*

As elucidated in previous sections, in the absence of any anomalies, no signals are reflected back to the transducer. Notwithstanding, the presence of an aberration causes the transmitted signal to be deflected back to the transmitting transducer, following a pulse-echo methodology. This phenomenon is illustrated in Figure 8 (Left), wherein the signal experiences deflection due to the influence of an anomaly either at or in proximity to the defect area, with a recorded time-of-flight amounting to 197.0 µs.

In the experimental study under consideration, three distinct types of deflections were examined: the hole, the bend, and the dent, referred to numerically as 1, 2, and 3, as depicted in Figure 8 (Right). Upon closer scrutiny, it was observed that only the signal from defect number 1 (the hole) could be discerned using the existing 48 kHz transducer. Regrettably, the signals pertaining to the other two types of deflections, the bend and the dent, remained undetected, largely due to the magnitude of the signal reflected by the first defect. It is suggested that for the purpose of generating signals over longer distances, a transducer with a lower frequency, ideally less than 10 kHz, should be employed. As illustrated in Figure 11, the signal reflected from defect number 1 could be successfully detected.

The method's inability to detect all defects arises from its reliance on guided ultrasonic surface waves across the W-Beam guardrail. These waves interact differently with various defect types, leading to variations in signal reflection. The specific reason lies in the geometry and material properties of different defects. For instance, bends (gradual deformations or curvatures in the rail head) may not cause significant signal reflection due to their smoother geometry. Similarly, dents (localized depressions or irregularities) can scatter or absorb USWs, making their detection challenging. This limitation significantly affects the method's practical applicability, emphasizing the need for further research, optimized transducer selection, signal transmission and amplification in signal detection in rail infrastructure safety.

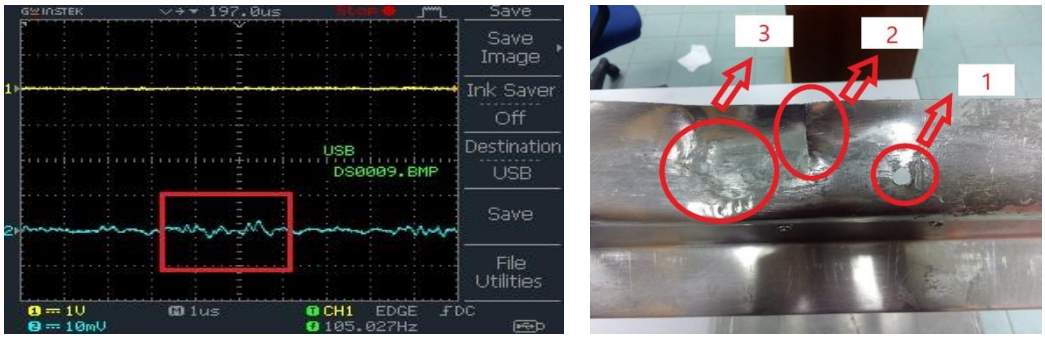


**Figure 8** Reflected signal that shows the defect at position 197.0 µs (Left) and the equivalent - defect (hole) detected by the reflected signal

3.2. Defect Position

In order to enhance the proficiency of the system in defect detection within the W-beam guard rail, it is imperative to ascertain the precise location of the defect. Given that the velocity of sound within the W-beam guard rail and the angle block is predetermined, the time-of-flight (t-o-f) for the defect signal can be discerned utilizing the signal

displacement within the scope, as exemplified in Figure 9. It is postulated that the time-distance correlation is linear, thereby facilitating the extrapolation of the actual defect location from the t-o-f.

The oscilloscope employed within this investigation, GWINSTEK GDS-1072-U, possesses a feature common to most of its kind - the capacity to pinpoint the location of a signal at a specific, desired position. Figure 9 (Left) illustrates that the current position is established at 180.0 µs for the signal's complete transmission. Consequently, any signal that emanates beyond the 180 µs mark is considered a reflected signal and could potentially signify a defect. A traversal across the horizontal axis reveals a reflected signal at a t-o-f position of 197 µs, as illustrated in Figure 9 (right), which could suggest the presence of a defect within the W-beam.

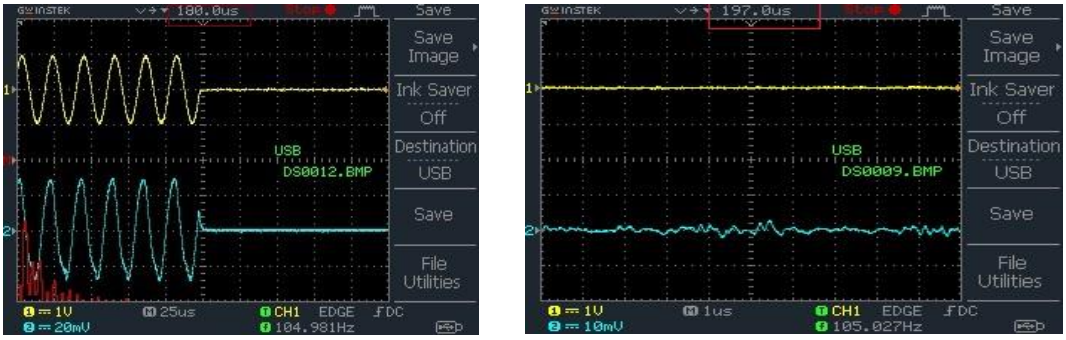


**Figure 9** The red box shows the position of the signal. Current (Left) Reflected (Right)

Nevertheless, this particular feature facilitates the identification of defect positioning, utilizing the principle of time-of-flight. The localization of the defect within the W-beam guard rail assumes paramount importance. By harnessing the defect's position delineated on the oscilloscope, it is possible to discern the tangible physical position of the defect on the guard rail. As depicted in Figure 13, the initiation of reflected signal transmission commences at position 180.0 µs onwards, with the defect detection site pinpointed at 197.0 µs. Utilizing this value positioning, the precise location of the defect, denoted as $L_{defect}$, can be accurately determined by applying Equation 4:

$$L_{defect} = \frac{t_a - t_b}{2} v_a \tag{4}$$

Where $t_a$ is the start time of the reflected signal transmission, $t_b$ is the position of the defect detected and $v_a$ is the speed of sound in aluminium.

Upon analysing the received signal, the substitution of Equation 5 with designated variables: $t_b$ = 197 µs, $t_a$ = 180 µs and $v_a$ = 6300 $ms^{-1}$, yields a calculated distance placing the defect at an approximate 5 mm from the transducer.

To substantiate this measurement, a comprehensive physical inspection is necessitated. Upon conducting the physical inspection, the actual defect location, as depicted in Figure 10, suggests that the type 1 defect (hole) is situated at a distance of 5 cm from the transducer. This observation unequivocally suggests the potential for long-distance detection in the context of w-beam guard rails utilized in road infrastructure.

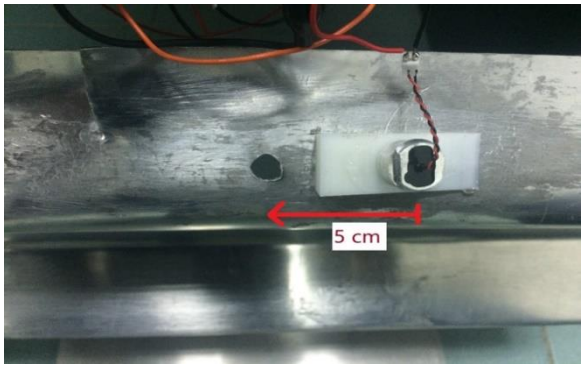


**Figure 10** Location of the defect is 5 cm away from the signal transmission

## 4.0 CONCLUSION

This research suggests the potential of employing an ultrasonic sensor network for long-distance defect detection in the ubiquitous W-beam guard rail across various road networks. A crucial prerequisite for ensuring road safety is the provision of a fully fastened guard rail. The empirical measurements derived from this study validate the feasibility of detecting holes in the guard rail, which could indicate the absence of a screw. A crucial factor in achieving efficient defect detection lies in selecting an appropriate frequency and wavelength. This choice is informed by the inherent variability in defect types, their distances, sizes, and the specific W-beam guardrail configuration. While empirical measurements on a single guardrail assume homogeneity within the guardrail population, a deeper understanding of precision and reliability can be gained by incorporating diverse types of W-beam guardrails. This cogent aspect warrants further investigation. Additionally, the choice of transducer setup could significantly enhance the quality of detection. In the context of this study, a pulse-echo setup was employed, utilizing a 10-cycle tone burst at a centre frequency of 48 kHz as the transmitter. The analysis of the received signal reflected by the specimen indicated that the proposed method could not detect all types of defects. However, it has been demonstrated that it is feasible to isolate the precise location of the physical defect based on the time-of-flight and standard textbook speed of sound velocities in materials. This discovery undoubtedly paves the way for significant improvement in global road safety measures.

## Conflicts of Interest

The authors declare that there are no conflicts of interest regarding the publication of this paper.


## Acknowledgement

The authors wish to acknowledge the Department of Mechatronics Engineering for supporting this work.


## References


[1] Marzougui, D., Mohan, P., & Kan, S. (2007). Evaluation of Rail Heights Effects on the Safety Performance of W - Beam Barriers. FHWA/NHTSA National Crash Analysis Center, 4(November), 1–30.

[2] Wilde, K., Bruski, D., Burzyński, S., Chróścielewski, J., Pachocki, & Witkowski, W. (2021). On analysis of double-impact test of 1500-kg vehicle into w-beam guardrail system. Archives of Civil Engineering, 67(2), 101–115. https://doi.org/10.24425/ace.2021.137157

[3] Reid, J. D., Kuipers, B. D., Sicking, D. L., & Faller, R. K. (2009). Impact performance of W-beam guardrail installed at various flare rates. International Journal of Impact Engineering, 36(3), 476–485. https://doi.org/10.1016/j.ijimpeng.2008.08.006

[4] Sheikh, N. M., & Bligh, R. P. (2013). In-field Inspection Methodology for Weathering Steel W-bean Guardrail. Texas A&M Transportation Institute - Report No 405160-29, 40, 5129–5160.

[5] I. Abdul Hamid, S.T.M. Syed Tajul Arif, N.S. Mohd Zulkiffli, R. Sarani, M.S. Solah, & M.R. Osman. (2017). Crash Investigation on Automobile vs. Crash Barrier: Assessment of W-Beam Guardrail with respect to REAM Standard. Journal of the Society of Automotive Engineers Malaysia, 1(2), 154–165. https://doi.org/10.56381/jsaem.v1i2.18

[6] Dutta, P. K. (2003). An investigation into the design and manufacture of FRP composite W-beam guardrail. International Journal of Materials and Product Technology, 19(1/2), 130. https://doi.org/10.1504/IJMPT.2003.003547

[7] Fredriksson, G., & Holmen, H. G. (2014). *Functional limits of the W-beam safety barrier*.

[8] Matthews, M. C. (1996). The use of surface waves in the determination of ground stiffness profiles. Proceedings of the Institution of Civil Engineers: Geotechnical Engineering, 119(2), 81–95. https://doi.org/10.1680/igeng.1996.28168

[9] Gregoire, D. J., & Kabakian, A. V. (2011). Surface-wave waveguides. IEEE Antennas and Wireless Propagation Letters, 10, 1512–1515. https://doi.org/10.1109/LAWP.2011.2181476

[10] Fitzgerald, W. J. (2008). *W-Beam Guardrail Repair: A Guide for Highway and Street Maintenance Personnel*. United States. Federal Highway Administration. Office of Safety.

[11] Ray, M. H., Engstrand, K., Plaxico, C. A., & McGinnis, R. G. (2001). Improvements to the Weak-Post W-Beam Guardrail. Transportation Research Record: Journal of the Transportation Research Board, 1743(1), 88–96. https://doi.org/10.3141/1743-12

[12] Sheikh, N., & Bligh, R. (2022). Evaluation of W-Beam Guardrail and Terminal Posts Installed in Metal Sleeves. Transportation Research Record, 2676(7), 355–362. https://doi.org/10.1177/03611981221078567

[13] Ham, S., Song, H., Oelze, M. L., & Popovics, J. S. (2017). A contactless ultrasonic surface wave approach to characterize distributed cracking damage in concrete. Ultrasonics, 75, 46–57. https://doi.org/10.1016/j.ultras.2016.11.003

[14] Fan, Y., Dixon, S., Edwards, R. S., & Jian, X. (2007). Ultrasonic surface wave propagation and interaction with surface defects on rail track head. NDT and E International, 40(6), 471–477. https://doi.org/10.1016/j.ndteint.2007.01.008
[15] Christensen, K. H., Röhrs, J., Ward, B., Fer, I., Broström, G., Saetra, Ø., & Breivik, Ø. (2013). Surface wave measurements using a ship-mounted ultrasonic altimeter. Methods in Oceanography, 6, 1–15. https://doi.org/10.1016/j.mio.2013.07.002
[16] Li, M., Anderson, N., Sneed, L., & Maerz, N. (2016). Application of ultrasonic surface wave techniques for concrete bridge deck condition assessment. Journal of Applied Geophysics, 126, 148–157. https://doi.org/10.1016/j.jappgeo.2016.01.020
[17] Dutton, B., Clough, A. R., Rosli, M. H., & Edwards, R. S. (2011). Non-contact ultrasonic detection of angled surface defects. NDT and E International, 44(4), 353–360. https://doi.org/10.1016/j.ndteint.2011.02.001
[18] R.Selfridge, A. (1985). Plastic Material's acoustic properties. IEEE Transactions On Sonics and Ultrasonics.
[19] Heavy, G. F. (2014). *Sound velocity table*. Class Instrumentation Ltd.